An Adaptive Grid Approach for the Simulation of Electromigration Induced Void Migration

H. Ceric and S. Selberherr

Institute for Microelectronics, TU Vienna
Gusshausstrasse 27–29, Vienna, Austria
Email: Ceric@iue.tuwien.ac.at

Abstract − **For tracking electromigration induced evolution of voids a diffuse interface model is applied. We assume an interconnect as two-dimensional electrically conducting via which contains initially a circular void. The diffuse interface governing equation was solved applying a finite element scheme with a robust local grid adaptation algorithm. Simulations were carried out for voids exposed to high current.**

I. INTRODUCTION

Failure of metallic interconnects in integrated circuits caused by electromigration has long been a key reliability concern which is further accentuated by the continuing trend of miniaturization. The phenomenon of electromigration is a mechanism for transport of matter by high electric current densities which produce damage in the interconnect lines. Failure results either from voids growing over the entire line width or extrusions which cause short circuits to neighboring lines.

Modeling the micromechanics of void evolution is a long-standing scientific problem. It began with sharp interface models requiring an explicit finite element tracking of void surfaces during the course of evolution [1, 2]. Later, prompted by the complexity of void surfaces, diffuse interface models were introduced [3]. Diffuse interface models circumvent computationally costly explicit surface tracking by application of a smooth order parameter field for representation of void structures. An alternative diffuse interface model based on the double obstacle potential was proposed in [4] where the computation is simplified by reduction of order parameter profiles evaluation only to void-metal interfacial area.

The main disadvantages of these diffuse interface models is their requirement of structured underlaying grids in order to build up grid for order parameter evaluation and also their restricted facility to reach higher resolution of an order parameter profile in the void-metal interfacial area. To overcome these drawbacks we solve the diffuse interface model governing equation with a finite element scheme coupled with a powerful grid adaptation algorithm. The robustness of the developed finite element approach with respect to the underlying grid structure makes it possible to efficiently simulate the damage induced by electromigration in complex interconnect geometries.

II. APPLIED DIFFUSE INTERFACE MODEL

We assumed unpassivated monocrystal isotropic interconnects where stress phenomena can be neglected. An interconnect is idealized as two-dimensional electrically conducting via which contains initially a circular void. For simplicity we also neglect the effects of grain boundaries and lattice diffusion. In this case there are two main forces which influence the shape of the evolving void interface: the chemical potential gradient and electron wind. The first force causes self-diffusion of metal atoms on the void interface and tends to minimize energy which results in circular void shapes. The electron wind force produces asymmetry in the void shape depending on electrical field gradients. In the diffuse interface models void and metal area are presented through the order parameter ϕ which takes values $+1$ in the metal area, -1 in the void area and $-1 < \phi < +1$ in the void-metal interface area. The model equations for the void evolving in an unpassivated interconnect line are for the order parameter [4],

$$\frac{\partial \phi}{\partial t} = \frac{2D_s}{\epsilon \pi} \nabla \cdot (\nabla \mu - |e|Z^* \nabla V) \tag{1}$$

$$\mu = \frac{4\Omega \gamma_s}{\epsilon \pi} (f'(\phi) - \epsilon^2 \Delta \phi) \tag{2}$$

and for the electrical field

$$\nabla \cdot (\sigma(\phi)\nabla V) = 0 \tag{3}$$

where D_s is the surface diffusivity, μ is the chemical potential, Z^* is the effective valence, e is the charge of an electron, γ_s is the surface energy, Ω is the volume of an atom, $f(\phi)$ is the double obstacle potential as defined in [4], ϵ is a parameter controlling the void-metal interface width and V is the electrical potential. The electrical conductivity was taken to vary linearly from the metal ($\sigma = \sigma_{metal}$) to the void area ($\sigma = 0$) by setting $\sigma = \sigma_{metal}(1+\phi)/2$. The equations (1) and (3) are solved on the two-dimensional polygonal interconnect area T.

III. NUMERICAL IMPLEMENTATION

The equations (1)-(3) are solved by means of the finite element method on the sequence of the grids $\Lambda_h(t_0 = 0), \Lambda_h(t_1), \Lambda_h(t_2)$ each one adapted to the position od the void-metal interface from the previous time step. The initial grid $\Lambda_h(0)$ is produced by refinement of some basic triangulation T_h of area T according to the initial profile of order parameter ϕ. The motivation of grid adaptation is to construct and maintain a fine triangulated belt of width $\epsilon\pi$ in the interconnect area where $-1 < \phi < +1$, respectively where void-metal interface area is placed.

a) Setting of the initial order parameter profile and initial grid refinement $\Lambda_h(0)$

The initial order parameter profile depends on the initial shape of the void $\Gamma(0)$ and can be expressed as

$$\phi(x,y) = \begin{cases} +1 & \text{if } d > \frac{\epsilon\pi}{2}, \\ \sin(\frac{d}{\epsilon}) & \text{if } |d| \le \frac{\epsilon\pi}{2}, \\ -1 & \text{if } d < -\frac{\epsilon\pi}{2} \end{cases} \tag{4}$$

Where $d = dist(P(x,y), \Gamma(0))$ is the signed normal distance of the point from the initial interface $\Gamma(0)$. To obtain sufficient resolution of this initial profile, the basic grid T_h is transformed into grid $\Lambda_h(0)$ obeying the following *initial grid refinement criterion (IMRC)* for the circular void with center O and radius r:

$$\forall K \in T_h \quad \text{if} \quad |dist(C_K, O) - r| \le \frac{\epsilon\pi}{2}$$
$$\text{than} \quad h_K < \frac{\epsilon\pi}{n} \tag{5}$$

n is the chosen number of grid elements across the void-metal interface width, h_K is the longest vertex of the triangle K, and C_K is its center of gravity. Now an adaptive algorithm defined in Section $c)$ transforms the basic grid T_h into initial grid $\Lambda_h(0)$ according to $IMRC$.

b) Finite element scheme

Let $\Lambda_h(t_n)$ be a triangulation of the area T at the discrete time t_n, and let $\{\phi_i^{n-1}\}_{i=0}^{N-1}$ be discrete nodal values of the order parameter on this triangulation. A finite element based iteration for solving (1) on grid $\Lambda_h(t_n)$ and evaluating the order parameter at the time $t_{n+1} = t_n + \Delta t$ consists of two steps [5]:
Step 1. For the kth iteration of $n + 1^{th}$ time step the linear system of equations has to be solved:

$$\epsilon\frac{\pi}{2}M_{ii}\phi_i^{n+1,k} + \Delta t D_s K_{ii}\mu_i^{n+1,k} = \alpha_i \tag{6}$$

$$M_{ii}\mu_i^{n+1,k} - \tau\left(\frac{1}{\epsilon}M_{ii} + \epsilon K_{ii}\right)\phi_i^{n+1,k} = \beta_i, \tag{7}$$

where

$$\alpha_i = \epsilon\frac{\pi}{2}M_{ii}\phi_i^n - \Delta t D_s \sum_{i \ne j} K_{ij}\mu_j^{n+1,k-1} \tag{8}$$

$$\beta_i = \tau\epsilon\sum_{i \ne j} K_{ij}\phi_j^{n+1,k-1} - |e|Z^* M_{ii}V_i^n \tag{9}$$

for each $i = 0, N - 1$ of the nodal values $(\phi_i^{n+1}, \mu_i^{n+1})$ of the triangulation $\Lambda_h(t_n)$. $[M]_{ij}$ and $[K]_{ij}$ are the lumped mass and stiffness matrix, respectively and $\tau = \frac{4\Omega\gamma_s}{\pi}$.
Step 2. All nodal values $\{\phi_i^{n+1}\}_{i=0}^{N-1}$ are projected on $[-1,1]$ by a function

$$\rho(x) = max(-1, min(1, x)). \tag{10}$$

For solving (3) a conventional finite element scheme is applied [6].

c) Maintaining the grid during simulation

After an order parameter was evaluated on the $\Lambda_h(t_n)$ a grid needs to be adapted according to the new void-metal interface position. Therefore it is necessary to extract all elements which are cut by the void-metal interface in grid $\Lambda_h(t_n)$. The following condition is used: Let us take a triangle $K \in \Lambda_h(t_n)$ and denote its vertices as P_0, P_1, P_2. The triangle K belongs to the interfacial elements if for the values of the order parameter ϕ at the triangle's vertices holds $\phi(P_0)\phi(P_1) < 0$ or $\phi(P_1)\phi(P_2) < 0$. We assume that an interface intersects each edge of the element only once. The set of all interfacial elements at the time t_n is denoted as $E(t_n)$. The centers of gravity of each triangle from the $E(t_n)$ build the interface point list $L(t_n)$. The distance of the arbitrary point Q from $L(t_n)$ is defined as

$$dist(Q, L(t_n)) = \min_{P \in L(t_n)} dist(Q, P). \tag{11}$$

Thus we can define the *transitional grid refinement criterion TMRC*

$$\forall K \in T_h \quad \text{if} \quad dist(C_K, L(t_n)) \le \frac{\epsilon\pi}{2}$$
$$\text{than} \quad h_K < \frac{\epsilon\pi}{n} \tag{12}$$

The grid adaption for the next time step evaluation of the order parameter ϕ is now completed with respect to $TMRC$ by as defined in the next section.

Figure 1: Atomic refinement operation.

d) Grid adaptation

The grid adaption algorithm used in this work is a version of the algorithm introduced in [7] and consists of a *grid refinement algorithm* and a *grid coarsening*

algorithm. The refinement algorithm is based on recursive bisecting of triangles. A triangle is marked for refinement if it complies with the refinement criterion $COND \in \{IMRC, TMRC\}$. For every triangle of the grid, the longest one of its edges is marked as *refinement edge*. The element and its neighbor element which also contains the same refinement edge are refined by bisecting this edge (Fig. 1). We can define refinement of the element in the following way:

Algorithm 1. *refinement of the element*
```
subroutine recursive_refine(element,COND)
{
  if neighbor has no compatible ref_edge
  recursive_refine(COND, neighbor)
  bisect(element)
  bisect(neighbor)
}
```

Now, the overall refinement algorithm can be formulated as follows:

Algorithm 2. *refinement of the grid*
```
subroutine refine_grid(COND)
{
  for n ≤ max_refinement_depth
  {
    for all elements
    if (COND) mark element for refinement

    if no element is marked
    break refinement loop

    for all elements
    recursive_refine(element,COND)
  }
}
```

The parameter max_refinement_depth limits the number of bisecting of each triangles of the grid. The grid is refined until there is no more element marked for refinement or the maximal refinement depth is reached.

The coarsening algorithm is more or less the inverse of the refinement algorithm. Each element that does not fullfils criterion $COND$ is marked for coarsening. The basic idea is to find the father element whose refinement produced the element in consideration.

Algorithm 3. *coarsening of the element*
```
subroutine coarsen(element)
{
  get the element_father
  get the father_neighbor on ref_edge
  coarse the element_father
  coarse the father_neighbor
}
```

The following routine coarsens as many elements as possible, even more than once if allowed:

Algorithm 4. *coarsening of the grid*
```
subroutine coarsen_grid(COND)
{
  do
  {
    do_coarsen_once_more = false
    for all elements
    if (!COND)
    do_coarsen_once_more |= coarsen(element)
  } until do_coarsen_once_more is false
}
```

The complete adaption of the grid is reached by sequential invoking of the grid refinement and of the grid coarsening algorithm.

IV. RESULTS

In all simulations a circle was chosen as initial void shape. The resolution of the parameter ϕ profile can be manipulated by setting parameter n which is the mean number of triangles across the void-metal interface. On Fig. 2 initial grids for $n = 1$ and $n = 5$ are presented. We
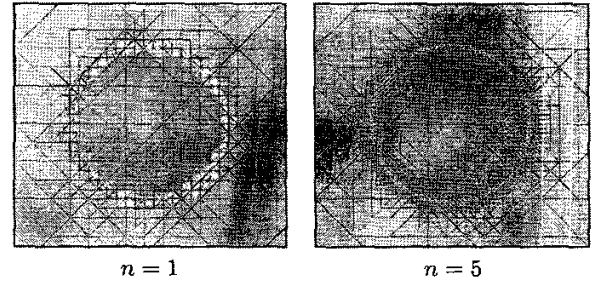

$n = 1$ $n = 5$

Figure 2: Initial grid refinements.

consider a two-dimensional, stress free, electricaly conducting interconnect via. A constant voltage is applied between points A and B (Fig. 3). At B a refractory layer is assumed. Because of geometrical reasons there is current crowding in the adjacencies of the corners C
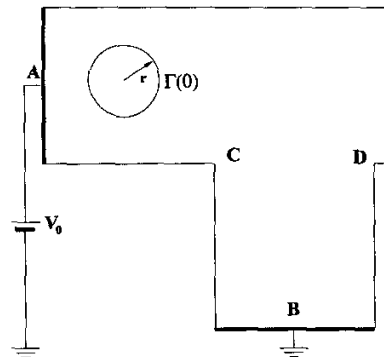

Figure 3: Interconnect via with initial void.

and D. The analytical solution of equation (3) has at these points actually a singularity [6], respectively. Due to current crowding in this area the influence of the electromigration force on the material transport on the void surface is more pronounced than the chemical potential gradient. This unbalance leads to higher asymmetry in the void shape then observed in the linear part of the interconnect. Our simulations have shown that voids follow the electrical current direction (Fig. 4) and do not transform in slit or wedge like formations which have been found to be a main cause for the complete interconnect failure [8].
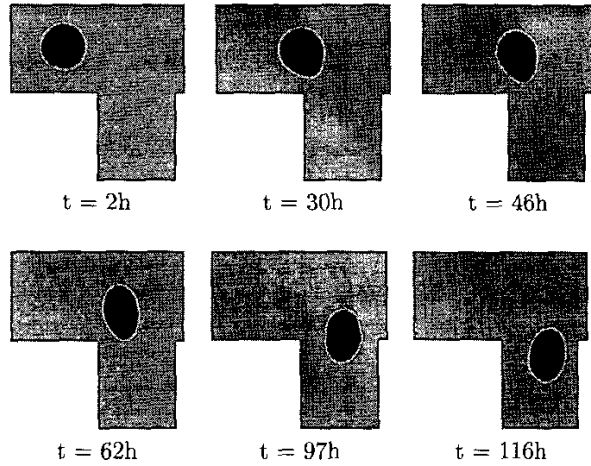

t = 2h   t = 30h   t = 46h

t = 62h   t = 97h   t = 116h

Figure 4: Void evolving through interconnect in the electric curennt direction

A fine triangulated belt area which is attached to the void-metal interface at the initial simulations step follows the interfacial area throughout the simulations whereby the interconnect area outside the interface is coarsened to the level of the basic grid T_h. The time step Δt is fitted at the simulations begin taking into account inverse proportionality of the speed of the evolving void-metal interface to the initial void radius [1]:

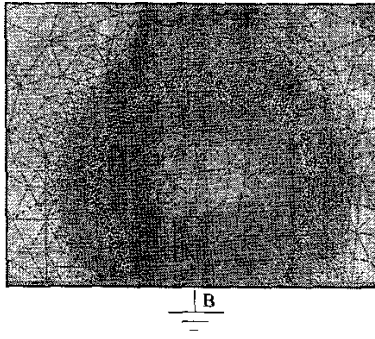$$\Delta t = \frac{\epsilon \pi r l}{2 D_s |e| Z^* V_0} \qquad (13)$$

Figure 5: Void collision with the refractory layer.

l is the characteristical length of via geometry. Appropriate choice of the time step ensures that the evolving void-metal interface will stay inside the fine grid belt during the simulation.

The capability of the adaptation scheme is also presented in the simulation of void collision with the interconnect refractory layer (Fig. 5).

V. CONCLUSION

A governing diffuse interface equation for the order parameter coupled with the Laplace equation for the electrical field is solved using the finite element scheme. A dynamically adapted grid is maintained by a refinement-coarsening algorithm controlled by position, curvature and width of the simulated void-metal interface which distributes the grid density in such a way that it allows an efficient simulation of evolving voids through large portions of complex interconnect geometry. Due to high electrical current gradients in the proximity of the interconnect corners and overall asymmetry of the electrical field, voids exhibit specific faceting which was not observed in the case of linear interconnect geometries. The applied diffuse interface model extends readily to incorporate additional physical phenomena such as anisotropy, temperature variations, and bulk and grain boundary diffusion.

ACKNOWLEDGMENT

REFERENCES

[1] D. R. Fridline and A. F. Bower, J. Appl. Phys. 85, 3168 (1999).

[2] M. R. Gungor and D. Maroudas, J. Appl. Phys. 85, 2233 (1999).

[3] M. Mahadevan and R. Bradley, Physica D 126, 201 (1999).

[4] D. N. Bhate, A. Kummar, and A. F. Bower, J. Appl. Phys. 87, 1712 (2000).

[5] C. Elliot and J. Ockendon, Weak and Variational Methods for Moving Boundary Problems (Pitman Publishing Inc., 1981).

[6] R. Sabelka, Dissertation, Technische Universität Wien, 2001.

[7] I. Kossacky, J. Comput. Appl. Math. 55, 275 (1994).

[8] E. Arzt, O. Kraft, W. D. Nix, and J. E. Sanchez, J. Appl. Phys. 76, 1563 (1994).